Incorporating Test Data for Small UAS at the Conceptual Design Level

Carl R. Russell
Colin R. Theodore
Aeromechanics Office
NASA Ames Research Center
Moffett Field, CA

Martin K. Sekula
Aeroelasticity Branch
NASA Langley Research Center
Hampton, VA

Increasing demand for improved capabilities of small unmanned aircraft systems (sUAS) has generated interest in improving the design techniques for these vehicles. sUAS have typically been designed using iterative methods with multiple prototypes, but advancements in aircraft design software will make it possible to generate conceptual designs of very small VTOL aircraft with reduced hardware prototyping. This paper describes a research effort to generate a conceptual design of an approximately 6-lb quadcopter using the NASA rotorcraft design software NDARC. Wind tunnel and hover test data are used to validate and refine the conceptual design results. The effects of parametric design variations on vehicle scale are shown. The design study described herein shows that the NDARC software, which was designed for full-scale rotorcraft, can be used to design and evaluate sUAS vehicles.

NOMENCLATURE

DGW	Design Gross Weight
NDARC	NASA Design and Analysis of Rotorcraft
sUAS	Small Unmanned Aircraft Systems
$c_{d,mean}$	Mean blade drag coefficient
C_T/σ	Thrust coefficient divided by solidity
P	Rotor power, HP
P_i	Rotor induced power, HP
P_o	Rotor profile power, HP
$\varkappa$	Rotor induced power factor, P_i/P_{ideal}
μ	Rotor advance ratio

INTRODUCTION

With the rapidly increasing popularity of multirotor small unmanned aircraft systems (sUAS), there has quickly emerged a demand for improved capabilities beyond those afforded by currently available vehicles. Specifically, operators are demanding vehicles that can fly farther, stay in the air longer, and carry heavier payloads. In general, much of the design work that has been done in the past on small multirotor aircraft has been accomplished with the "cut and try" method. For full-scale manned aircraft, this strategy is prohibitively expensive, but for small-scale sUAS, many design iterations can be prototyped and tested while incurring relatively minimal time and cost.

The Design Environment for Novel Vertical Lift (DELIVER) sub-project of NASA's Convergent Aeronautics Solutions Project [Ref. 1] seeks to apply the knowledge and tools developed over decades of full-scale rotorcraft research and apply them to sUAS design. The DELIVER project has supported sUAS research in multiple areas, including acoustics, autonomy, hybrid-electric and all-electric propulsion, performance modeling and testing, and conceptual design. The work covered in this paper is primarily concerned with performance modeling and testing and conceptual design.

Despite the relatively low cost of multiple design iterations for sUAS, the design process for this class of aircraft stands to benefit from improvements in predictive capabilities of aircraft design and analysis tools. By applying design strategies normally used for full-scale rotorcraft to sUAS, the design cycle for these vehicles should be shortened, while improving the capabilities of the designs. By studying the performance of currently available sUAS vehicles, models for vehicles at this scale can be developed that accurately predict performance and simulate trajectories. These models can then be used to size new vehicles with expanded capabilities.

Researchers have begun exploring the use of classical rotorcraft design and analysis tools for sUAS design and analysis. For example, Ref. 2 employed a dynamic simulation with a traditional rotor wake modeling approach to estimate the performance of a family of multirotor aircraft. Reference 3 used classical blade-element momentum theory to simulate the performance of sUAS rotors in order to optimize rotor performance. In Ref. 4, the rotorcraft comprehensive analysis software CAMRAD II was used to estimate sUAS rotor performance in hover using different levels of fidelity for the modeling of the rotor wake and the elastic blade properties.

The primary rotorcraft design tool used by NASA rotorcraft researchers is NDARC (NASA Design and Analysis of Rotorcraft, first described in Ref. 5). The NDARC toolchain has been extensively validated for full-scale rotorcraft, but

Presented at the AHS International Technical Conference on Aeromechanics Design for Transformative Vertical Flight, San Francisco, CA, January 16-18, 2018.

until recently, NDARC had not been used for sUAS-scale vehicles and configurations, such as multirotors. This paper discusses efforts to extend NDARC capabilities to sUAS by using measurements, such as wind tunnel test results and individual component weights and performance, to improve and validate current analytical models.

After the validation data are presented, results are shown for parametric variations of aircraft characteristics. These results show how sUAS vehicles can be expected to scale with quantities such as battery specific energy. Finally, some recommendations are given as to how NDARC or other conceptual design software should be used for future sUAS design activities.

METHODOLOGY

Following a description of the NDARC models, descriptions are given for the various elements of the conceptual design toolchain. Elements that are covered include detailed rotor geometry extraction, comprehensive analysis, wind tunnel validation data, and component weights and efficiencies.

Conceptual Design Software

The design software used for this study is NDARC. NDARC is a conceptual/preliminary design and analysis code for rapidly sizing and conducting performance analyses of new rotorcraft concepts. By using simplified models to represent major rotorcraft subsystems, such as engines and rotors, NDARC can produce multiple rotorcraft designs quickly without requiring repeated runs of time-intensive engine cycle or rotor performance analyses.

While the original function of NDARC was to model common full-scale rotorcraft configurations, such as helicopters and tiltrotors powered by turboshaft engines, the modular code base of the software allows its extension to various advanced concepts. These advanced concepts include, but are not limited to, hybrid/electric propulsion systems, distributed electric propulsion, and multirotor systems. Extensions of the NDARC software to include advanced propulsion systems are described in Ref. 6. A recent NASA design study used these latest propulsion-modeling capabilities of NDARC to model vehicles relevant to the emerging urban air mobility market. That study is described in Ref. 7, and focused on three advanced VTOL configurations using electric or hybrid-electric propulsion.

Like the research of Ref. 7, the study described herein exercised the advanced propulsion models of NDARC and its ability to model arbitrary configurations. While the primary tool used for this study was NDARC version 1.12, the software does not operate without significant tuning and input from various sources. The toolchain and process that was used for this design study is shown in Fig. 1.

The following sections describe the elements of Fig. 1 and how they were applied to the conceptual design process for this work.

Rotor Blade Geometry

Rotor blade geometries were extracted using a laser scanner, and the geometry extraction process is more fully described in Ref. 4. From a 3-dimensional model of the rotors, airfoil geometries were obtained along with planform characteristics, such as twist and chord distribution. The FUN3D CFD software used the airfoil geometries to generate airfoil tables, which were then used by CAMRAD II along with the rotor planform characteristics to compute rotor performance.

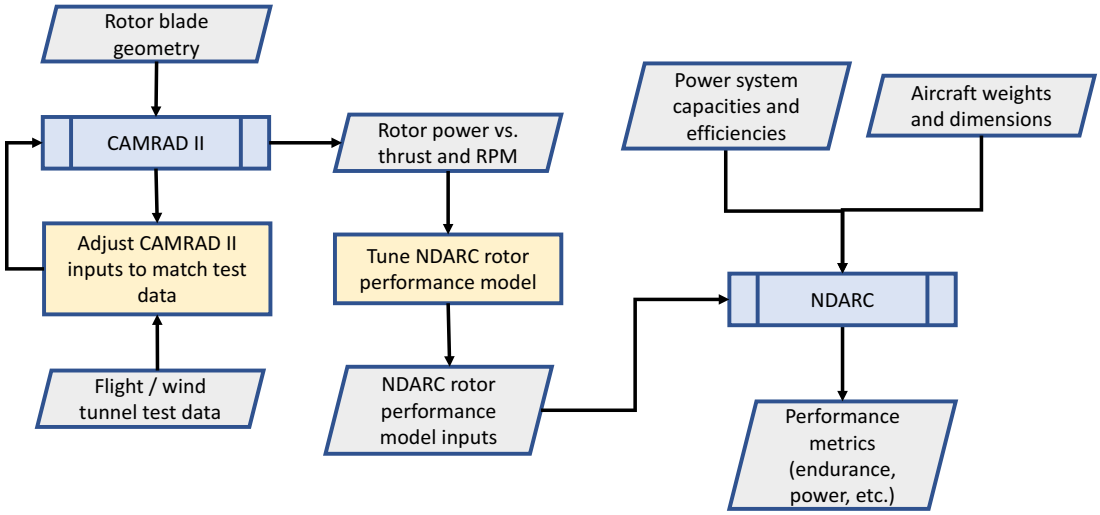

Figure 1. NDARC and CAMRAD II modeling toolchain for sUAS

Comprehensive Analysis

The CAMRAD II comprehensive analysis code was used to model the UAS rotor system loads and performance. These models were used to develop performance databases for a range of flight conditions, which in turn were used to train the NDARC rotor performance models.

The development of CAMRAD II models requires a geometric description of the UAS rotor being modeled. The major inputs into the analysis include the blade planform (spanwise chord distribution), spanwise blade twist, and spanwise airfoil distribution. These parameters were obtained from a laser scan of the rotor. Typically, the blade is modeled as a rigid beam; therefore, estimates of the structural parameters are not required, and neglecting flexibility and associated aeroelastic phenomena is a reasonable approximation [Ref. 4]. While most sUAS rotors utilize RPM control to vary thrust, CAMRAD II models of these rotors are developed with a pitch bearing to provide a simple means of adjusting the blade pitch index to more closely match experimental data.

There are numerous aerodynamic modeling options of varying fidelity available for simulating the aerodynamic loads produced by sUAS rotors. CAMRAD II has several inflow modeling options in its aerodynamic analysis, ranging from simple uniform inflow to free wake to external CFD. Most of these models require the use of airfoil tables (c81 format) to provide lift, drag, and pitching moment coefficients as a function of Mach number and angle of attack. For the purposes of modeling small-scale UAS rotors, a 2-dimensional CFD analysis is employed to develop these tables for various airfoil sections across the blade span. Potential flow methods, such as XFOIL, were capable of providing reasonable aerodynamic coefficient predictions over a limited range of conditions and portions of the rotor blade. These limitations were due to issues such as blade stall, Reynolds number effects, and large, blunt trailing edges relative to the blade thickness. The latter of these is a directly related to the manufacturing limitations of small-scale rotors. Utilizing potential flow methods is a tradeoff between accuracy and computational cost and should be weighed accordingly.

Generally speaking, multiple airfoil tables should be defined across the span of the rotor blade [Ref. 4] since most sUAS rotors have a constantly-varying blade cross-section. Choice of inflow model has been shown to have some influence on thrust and rotor power, but the only configuration-independent trend identified is that the free-wake model appears to produce a more-realistic lift distribution across the blade.

Experimental Performance Data

To better understand the performance characteristics of multirotor sUAS, two wind tunnel tests were performed in the U.S. Army's 7- by 10-ft wind tunnel at Ames Research Center. The first, executed in late 2015, was documented in Ref. 8. The second test, in early 2017, used much of the same hardware and methodology as the first, but added two new vehicles, along with additional measurements, including blade deflection using photogrammetry and vibration measurements using high-speed collection of force and moment data. The data from these wind tunnel tests will be made publicly available for researchers wishing to validate their own calculations.

Much of the analysis presented in this paper is based on the Straight Up Imaging Endurance [Ref. 9], pictured in the wind tunnel in Fig. 2. The Endurance is an approximately 6-lb quadcopter with 15-in diameter rotors, and its primary design mission is aerial surveillance. The Endurance was tested in the wind tunnel in the full vehicle configuration, shown in Fig. 2. In addition, an isolated Endurance rotor was tested as well as the bare airframe in order to acquire better component performance data. The isolated rotor and complete vehicle were also tested in a hover configuration. These data were then used to validate the predictions made by both NDARC and CAMRAD II.

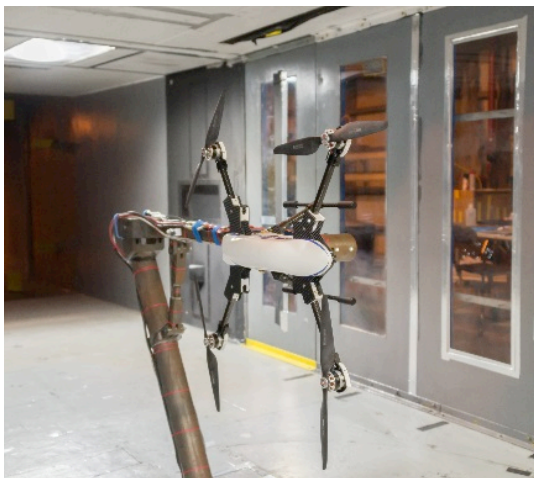

Figure 2. Straight Up Imaging Endurance installed in the 7- by 10-ft Wind Tunnel

NDARC Rotor Performance

NDARC uses a reduced-order rotor performance model to facilitate fast turn-around time of simulations. This performance model calculates the induced and profile components of the rotor power based on the mean blade drag coefficient, $c_{d,mean}$, and induced power factor, $\varkappa$. The values for $c_{d,mean}$ and $\varkappa$ are calculated in NDARC by parametric equations as functions of advance ratio, inflow, blade loading (C_T/σ), thrust offset, and tip speed.

The results of the CAMRAD II parameter sweeps are used to manually tune the NDARC performance equations. By matching the NDARC performance equations to the CAMRAD II output, good estimates of rotor power are obtained. Comparisons of NDARC rotor power calculations with CAMRAD II output and experimental data are provided in the Results section.

Small quadcopters use rigid rotors with adjustable RPM for flight control. The NDARC quadrotor model was set up using RPM control with three-variable symmetric trim to balance axial and vertical forces as well as pitching moment. The NDARC blade element model was exercised to determine the rotor forces and moments as a function of RPM, speed, and attitude. The non-linear twist and chord distribution obtained from the laser-scanned geometry were used as input to the blade element model. Blade stiffness was set arbitrarily high in order to suppress tip-path-plane tilt due to hub moments.

NDARC Component Models

NDARC has models for component weights and efficiencies, but the results of these models are only as good as the data used to calibrate them. For traditional rotorcraft, NDARC has curve fits based on extensive collections of data from existing aircraft. For aircraft such as the quadrotors modeled for this study, these collections of calibration data do not exist.

The component weight models contained in NDARC have a level of detail that is not appropriate for sUAS. For example, the rotor weight model is broken down into subcomponents, such as hub and hinge, blade assembly, and fairing/spinner. Because of the very simple one-piece design of sUAS rotors it is not possible to even determine where the hub stops and the blade begins. In addition, blade weight models based on spar-and-skin helicopter rotors are not appropriate at this small scale, where blade construction consists of either injection molded plastic or carbon-wrapped wood or foam.

NDARC version 1.12, which was used for this study, includes generic weight models for several subsystems, allowing the user to define component weights based on very minimal sets of parameters. For this design study, generic weight models were used for the rotors, fuselage, and motor components. Blade weight was based on a curve fit, shown in Fig. 3, to weights for six existing propellers of the type (T-Motor carbon fiber blades) used on the Endurance aircraft. The remaining component weights of the rotor, such as the hub weight, were set to zero. Based on the weights of these six propellers, the entire blade weight, W_{blade} (lb), was approximated as a function of rotor radius, R (ft):

$$W_{blade} = 0.1413R^{2.1324}$$

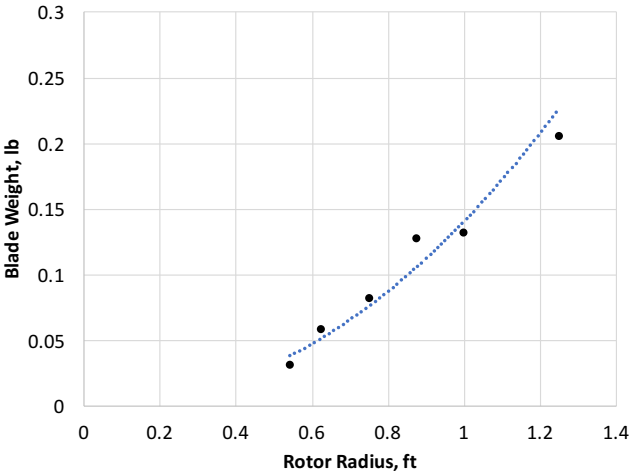

Figure 3. Blade weight curve fit

Similar trends were developed for the fuselage and motors and are shown in Figs. 4-5, respectively. The weights used for the fuselage models come from three different multirotor aircraft. The motor weight model is based on manufacturer specifications for five different motors in the same series as those used on the Endurance (T-Motor Navigator series). The fuselage was assumed to include all of the vehicle structure except for the motor supports and landing gear. The motor supports were assumed to be 1% of maximum takeoff weight, and landing gear weight was assumed to be 4% of design gross weight. The fuselage weight, W_{fus} (lb), was calculated as a function of design gross weight, DGW (lb):

$$W_{fus} = 354.52\left(\frac{DGW}{1000}\right)^{1.097}$$

All of the airframe drag was bookkept in the fuselage and was based on wind tunnel test results from Ref. 8. Because the bare airframe wind tunnel testing included the entire airframe, the drag buildup couldn't be further subdivided. Drag values for all airframe components other than the fuselage were set to zero.

Electric motor weight in general exhibits its strongest dependency on maximum torque. The torque-based weight model in NDARC was found to over-estimate the motor weights for electric motors at this small scale, so a different trend was developed for the work presented here. Motor weight, W_{motor} (lb) was approximated as a function of maximum torque, Q_{max} (ft-lb):

$$W_{motor} = 0.3256{Q_{max}}^{0.5017}$$

All systems weights were bookkept as a single fixed weight of 0.78 lb, based on the Endurance navigation system components (GPS, autopilot, etc.), which are typical of a sUAS quadcopter. Even though there is no transmission on

this type of aircraft using direct drive motors, NDARC requires a transmission component to distribute the motor power to the rotors. For each motor/rotor pair, an NDARC propulsion group was specified having zero weight and a gear ratio of 1.

All other component weights except for the battery were set to zero. Current hobby-grade LiPo batteries have stated energy densities of approximately 135 Wh/kg installed; however, users typically apply an "80 percent rule" and assume that only 80 percent of a battery's stated capacity is available for use. This rule of thumb gives an approximate specific energy of 110 Wh/kg. Compared with the energy densities being considered for manned-scale electric aircraft (Ref. 7 gives an installed specific energy of 93 Wh/kg for current technology), 110 Wh/kg is high. Note that sUAS batteries do not require the heat dissipation, battery management, and other hardware required for high capacity battery packs intended for use in larger scale aircraft.

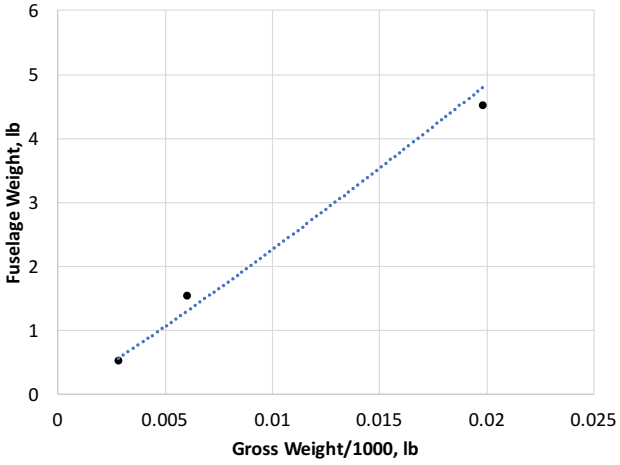

Figure 4. Fuselage weight curve fit

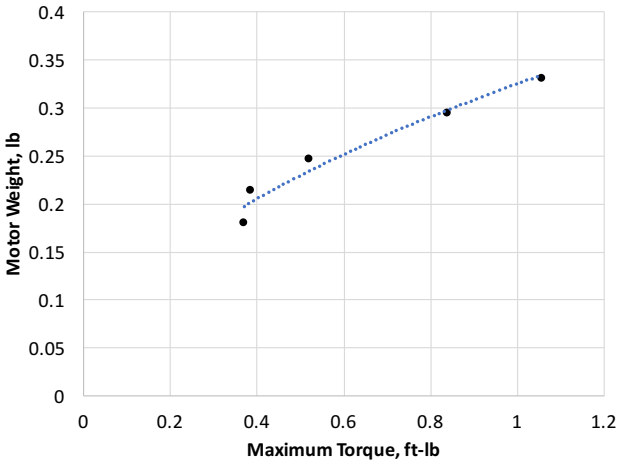

Figure 5. Motor weight curve fit

Multiple battery energy densities were considered, from the current technology value of 110 Wh/kg up to a maximum of 400 Wh/kg, installed. The effects of battery specific energy on vehicle design gross weight are shown in the Results section. Battery wiring was assumed to be 5% of battery weight. Battery discharge efficiency was assumed to be 98%. Based on results found in Ref. 8, combined motor and speed controller efficiency was 75%.

Sizing Study

Once the NDARC quadcopter model was set up and producing satisfactory results, a brief sizing study was conducted to determine the effects of changes in payload weight, battery specific energy, and mission length on DGW.

A simple baseline design mission was assumed, consisting of a single mission segment—20-minute hover out of ground effect carrying a 0.5 lb payload. Payloads up to 1 lb and mission times up to 1 hr were considered.

The only other sizing criteria was hover at sea-level standard conditions and 2.5 times design gross weight. A maximum thrust-to-weight ratio of 2.5 is typical for non-acrobatic quadcopters, so this condition was used to size the motors. The sizing study is discussed further in the Results section.

RESULTS

This section presents the results in the following format. First, CAMRAD II results are compared with the experimental data. Next, the results of the NDARC performance model tuning process are shown, followed by a comparison of the NDARC results with the experimental data. Finally, the results of parametric scaling runs are given, showing the impact of payload weight, battery specific energy, and mission length on vehicle design gross weight.

Comprehensive Analysis Results

Reference 4 gives a comparison of hover test data and CAMRAD II output for the isolated SUI Endurance rotor. Those results are repeated here in Figs. 6 and 7, followed by forward flight results in Figs. 8-10. The comprehensive analysis produces good results for sUAS rotors at this scale. The simulated rotor thrust is slightly below the experimental thrust in hover, while the simulated rotor power is very close to the experimental values.

For the forward flight thrust values at 40 ft/s shown in Fig. 8, three different vehicle pitch angles are shown. Other angles were tested and simulated, ranging from -40 to +40 deg, but a typical quadcopter will fly at a pitch angle between 0 and 10 deg. The results shown are therefore the most relevant to the work being presented here. The thrust variation with rotor RPM and forward flight speed is generally well predicted by CAMRAD II with a maximum error of approximately 10%.

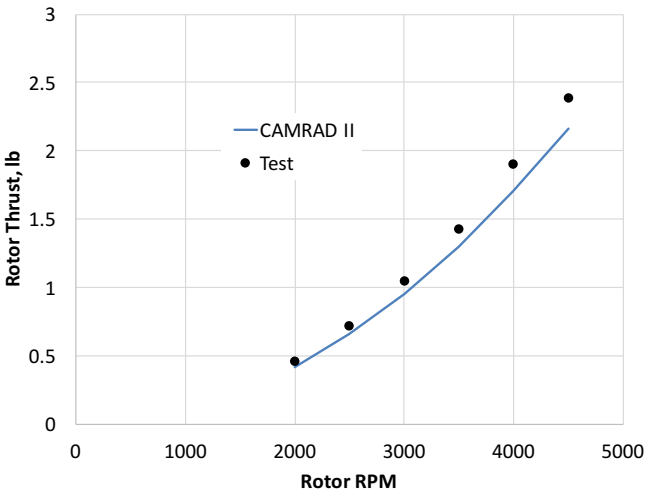

Figure 6. Isolated rotor thrust in hover – test vs. CAMRAD II

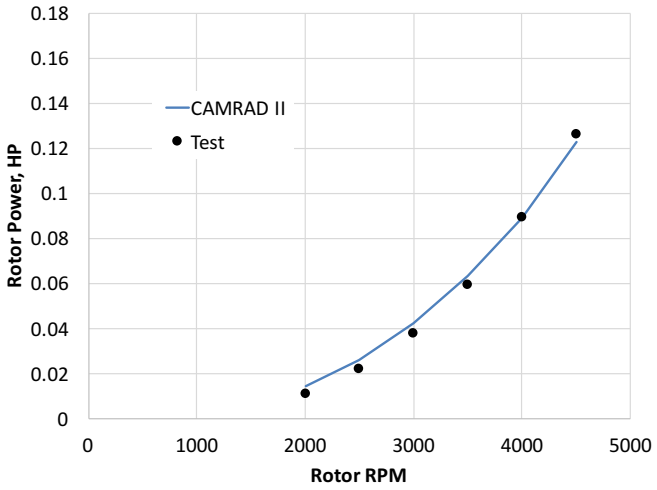

Figure 7. Isolated rotor power in hover – test vs. CAMRAD II

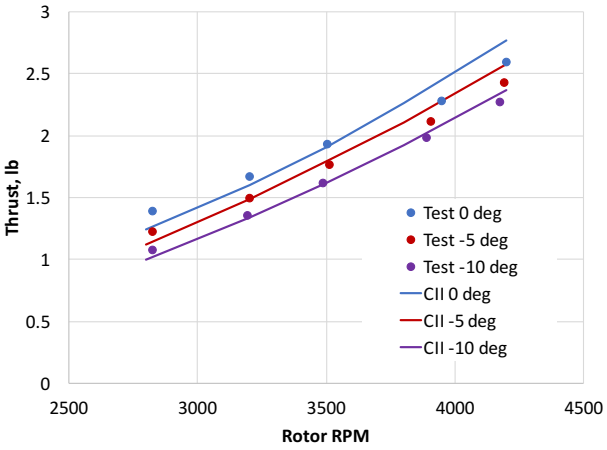

Figure 8. Isolated rotor thrust at 40 ft/s – test vs. CAMRAD II

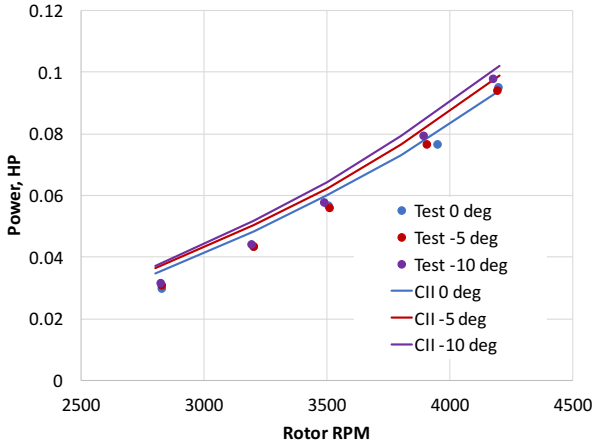

Figure 9. Isolated rotor power at 40 ft/s – test vs. CAMRAD II

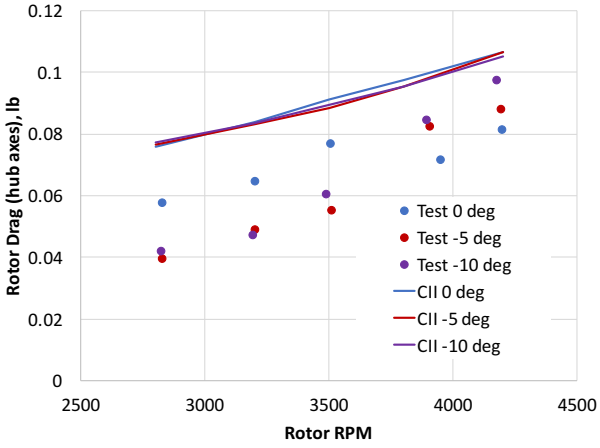

Figure 10. Isolated rotor drag at 40 ft/s – Test vs. CAMRAD II

The rotor power, shown in Fig. 9, is slightly over-predicted for all RPM values. The rotor drag shown in Fig. 10 is over-predicted by the comprehensive analysis when compared with the experimental data. These data do have a high degree of relative uncertainty due to the very small rotor drag values. The experimental uncertainty in the rotor drag is approximately 0.09 lb, so the CAMRAD II predictions fall well within the uncertainty bounds of the data. The trend of increasing drag with RPM is similar for both the analysis and experimental data.

NDARC Rotor Model Tuning

Based on the CAMRAD II results, the NDARC rotor performance model was tuned to match the values of $\varkappa$ and $c_{d,mean}$. For hover performance, rotor induced power only varies with blade loading, C_T/σ. Figure 11 shows the variation of the induced power factor, $\varkappa$, with rotor collective. As shown, the results do not vary with rotor RPM. Once tuned, the NDARC induced power model fit the CAMRAD II results over a wide range of rotor collective.

Figure 12 shows the variation of $c_{d,mean}$ with collective for three different rotor speeds for both the CAMRAD II output and the NDARC reduced-order model. The $c_{d,mean}$ results show the significant effect of Reynolds number on the profile power. At 3,500 rpm, the Reynolds number at 75% radius is approximately 50,000. At this very low Reynolds number, the profile drag coefficient of the blade airfoils decreases as Reynolds number increases. $c_{d,mean}$ is therefore higher for lower rotor speeds.

The NDARC profile power model does not include variation with Reynolds number, but it does include variation with tip Mach number. Typically, the profile power will begin to rise for tip speeds above Mach 0.8. Because the rotors studied here do not operate near sonic speeds, the tip Mach variation in the NDARC rotor power model was used instead to account for the profile power drop with increased rotor speed. As Fig. 12 shows, the calibrated $c_{d,mean}$ values closely match the CAMRAD II results for hover.

Matching the NDARC models for both induced and profile power with the CAMRAD II results was more difficult in forward flight. Figures 13 and 14 show values for $\varkappa$ and $c_{d,mean}$, respectively, for forward flight at three aircraft pitch angles, with negative values defined as nose down. Two forward flight speeds, 20 and 40 ft/s, were modeled, and the results are presented in terms of advance ratio. The plots are annotated to show the forward speeds and RPM values that correspond to the various advance ratios.

Matching the CAMRAD II results with the NDARC model for both 20 and 40 ft/s was not possible. Also, the results for $\varkappa$ and $c_{d,mean}$ are almost certainly inaccurate at 20 ft/s. The $\varkappa$ values are below 1 at this speed, which is not possible for a physical rotor, and the $c_{d,mean}$ values seem unreasonably high. This result is not unexpected, as it is typically very difficult for comprehensive analysis codes to accurately model rotor wakes for advance ratios below $\mu = 0.1$.

For the remainder of the study, $\varkappa$ and $c_{d,mean}$ were held constant with forward speed and inflow ratio. Because of the questionable accuracy of the $\varkappa$ and $c_{d,mean}$ values at low advance ratios, the hover performance values were judged to be accurate enough.

NDARC Rotor Performance

With all of the NDARC models calibrated, the next step was to compare the output of the sizing code against experimental data. Figures 15 and 16 show the hover thrust and power, respectively, computed by NDARC for a single rotor of the SUI Endurance compared with test results.

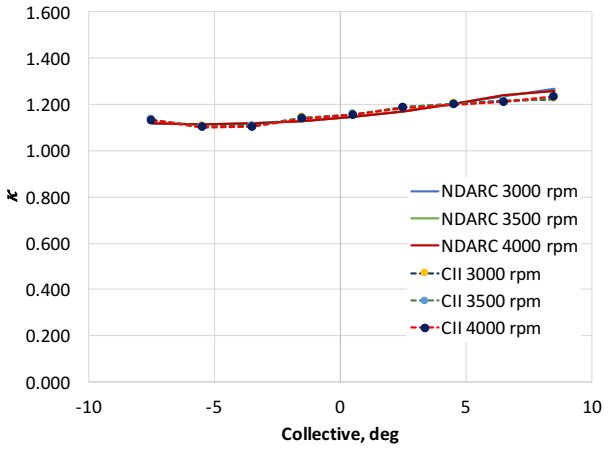

Figure 11. Fitting NDARC to CAMRAD II – induced power in hover

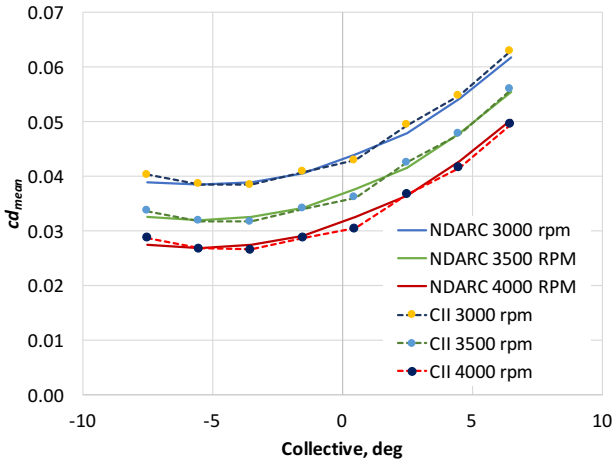

Figure 12. Fitting NDARC to CAMRAD II – profile power in hover

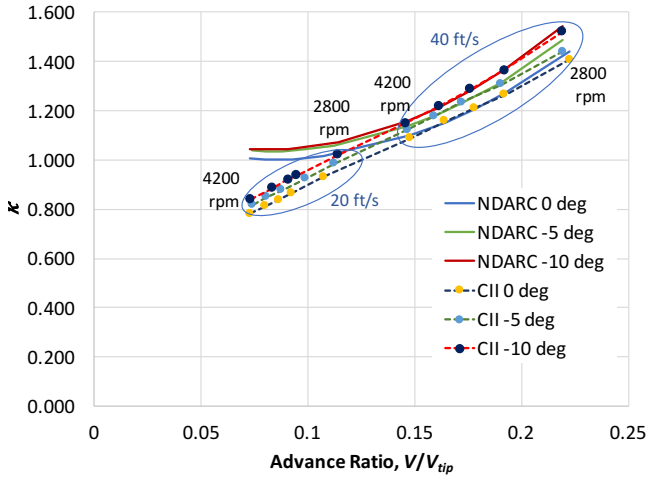

Figure 13. Fitting NDARC to CAMRAD II – induced power in forward flight

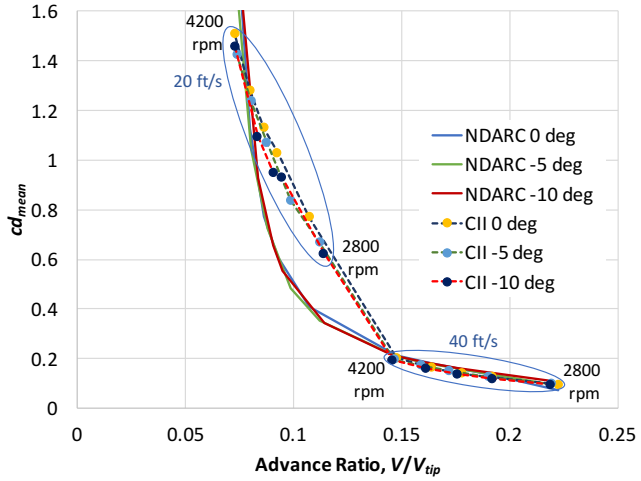

Figure 14. Fitting NDARC to CAMRAD II – profile power in forward flight

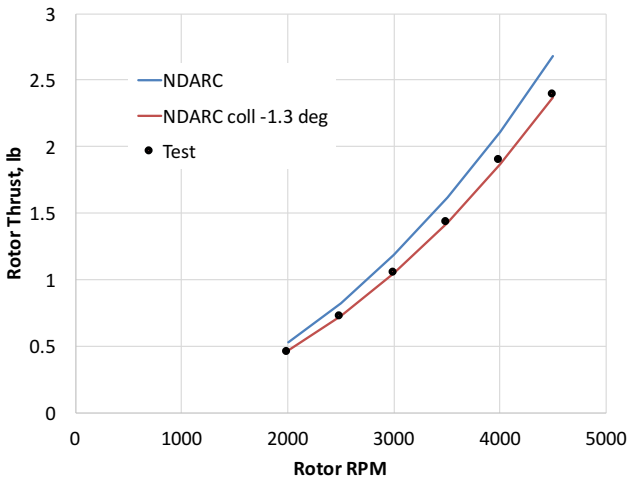

Figure 15. Isolated rotor thrust in hover – test vs. NDARC

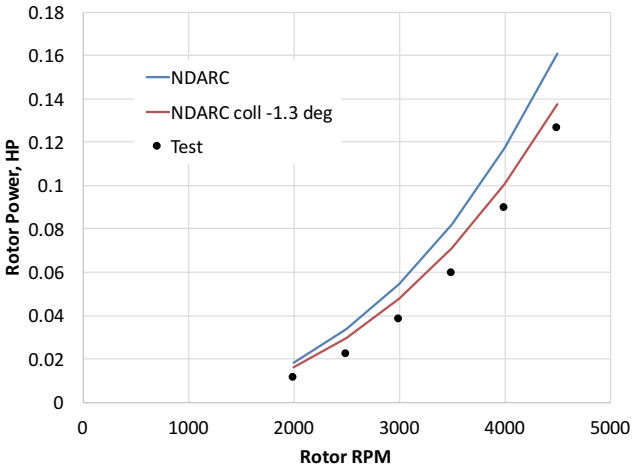

Figure 16. Isolated rotor power in hover – test vs. NDARC

The blue curves in Figs. 15 and 16 show the results that were computed by the NDARC blade-element model using the actual twist distribution of the Endurance rotor blade. The twist distribution includes the physical distribution measured by the laser scanning process as well as an estimate of zero-lift angle of attack. For the Endurance rotor blades, the zero-lift angle was approximated to be -3.4 deg, based on the FUN3D results for the airfoil nearest to 75% radius. Because the actual airfoil varies along the blade span, some error may be introduced by assuming a constant zero-lift angle of attack.

As shown in Figs. 15 and 16, both the thrust and power were over-estimated using the above method. The collective pitch angle was then adjusted by -1.3 deg to match the experimental thrust at 3,500 rpm, and the resulting thrust and power are included in Figs. 15 and 16. The adjusted hover thrust matches the experimental thrust very well for all rotor speeds tested, while power is still slightly over-estimated.

This result is consistent with those of Ref. 4 and Figs. 6 and 7, which showed that if predicted thrust is matched to test results, the power will be over-estimated. Since the NDARC inputs come from the CAMRAD II outputs, this outcome is expected, demonstrating that NDARC is properly capturing the computed values from CAMRAD II. Whether the source of the remaining discrepancy in the power calculation is in the comprehensive analysis implementation or in the underlying airfoil tables remains uncertain.

Compared to hover, the correlation of forward flight NDARC results and experimental data is not as good. Figures 17, 18, and 19 show a comparison at 40 ft/s of the NDARC and test results for isolated rotor thrust, power, and drag, respectively. These results were generated using the adjusted rotor collective of -1.3 deg. The thrust and power in forward flight were both over-predicted by approximately 10-20%. The rotor drag predicted by the blade-element model is significantly higher than the measured values – in some cases more than double. As with the CAMRAD II results, the rotor drag values generated by NDARC are still within the experimental uncertainty. Further study is needed to fully understand the discrepancies between the modeled values and experimental results.

Sizing Study Results

A brief sizing study was conducted to demonstrate how NDARC can be used to re-size a quadcopter given varying mission requirements. The baseline vehicle was partially modeled on the Straight Up Imaging Endurance, but was re-sized using the weight trends and rotor performance models described in the Methodology section. The resulting baseline vehicle is summarized in Table 1.

Figure 20 shows the power breakdown for the baseline vehicle as a function of speed. As described in the NDARC rotor performance results, the accuracy of the forward flight results may not be very good, but it is still useful to see whether the rotor power follows the typical trends for rotors in forward flight. As Fig. 20 shows, the power follows typical helicopter power trends, with a power bucket formed due to drop-off of induced power in low-speed forward flight and increased parasite and profile power at higher speeds.

Figure 21 provides values for the key trim variables as a function of forward speed. Because there is no flapping of the rotor blades, the rotor tip path plane and the resulting thrust vector can only be tilted by tilting the entire vehicle. Pitch angles are therefore significantly higher for the given speeds than would be expected for a vehicle using flapping rotors, with a speed of just 20 kt resulting in the nose being pitched down almost 7 degrees. Figure 21 also shows how rotor RPM varies as a function of forward flight speed. The vehicle center of gravity is slightly aft of its geometric center, leading to the higher rotor speed on the aft rotors in hover. In forward flight, additional differential thrust between aft and forward rotors is needed to maintain a downward pitch angle.

Finally, variations in mission time, payload weight, and battery specific energy were investigated to determine their effect on vehicle sizing. Figure 22 shows how design gross weight varies with mission time for a number of different battery energy densities with a 0.5-lb payload. The mission used to size the aircraft was a simple hover out of ground effect for a set amount of time. Current off-the-shelf battery

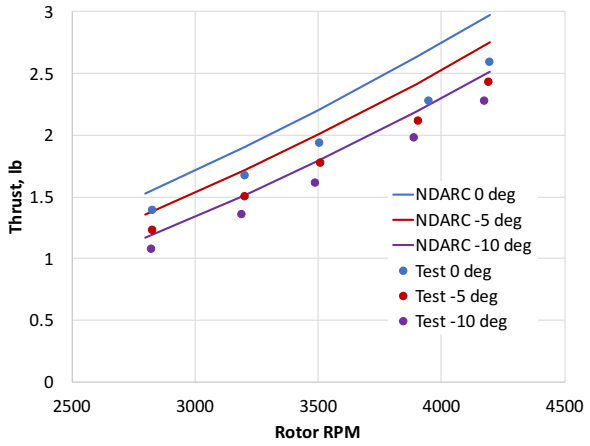

Figure 17. Isolated rotor thrust at 40 ft/s – test vs. NDARC

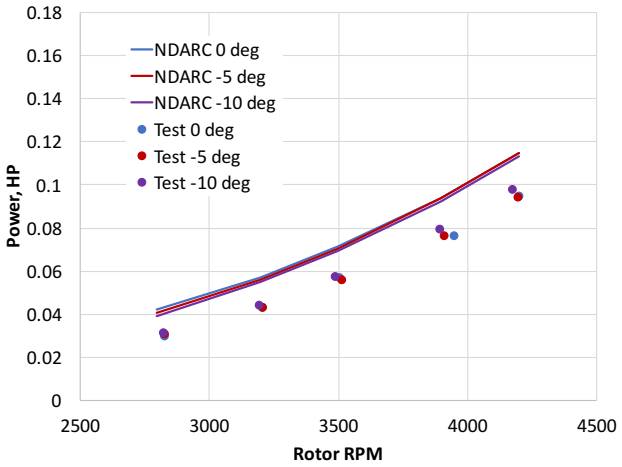

Figure 18. Isolated rotor power at 40 ft/s – test vs. NDARC

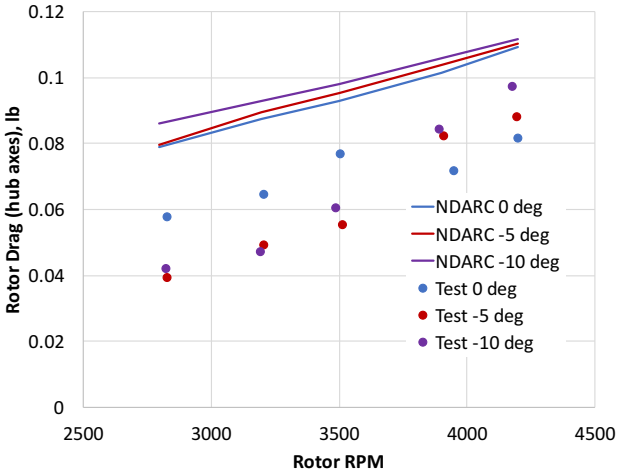

Figure 19. Isolated rotor drag at 40 ft/s – test vs. NDARC

Table 1. Baseline quadcopter design summary

Physical Characteristics		Vehicle Performance	
Disk Loading, lb/ft^2	1.22	Best Range Speed (V_{br}), kt	32.9
Rotor Solidity	0.095	Best Endurance Speed (V_{be}), kt	20.4
Rotor Radius, ft	0.644	Maximum Speed (V_{max}), kt	45.8
DGW, lb	6.35	Range, nm	39.3
Empty Weight, lb	5.85	Effective Lift-to-Drag at V_{br}	2.26
Battery+wiring, lb	2.28	Design C_T/σ	0.103
Airframe, lb	1.61	Hover Current, 1/hr	2.94
Rotors, lb	0.22	V_{br} Current, 1/hr	2.57
Motors, lb	0.72		
Systems, lb	0.78		
Power, HP/motor	0.29		
Battery Capacity, Wh	109.7		
Drag D/q, ft^2	0.30		

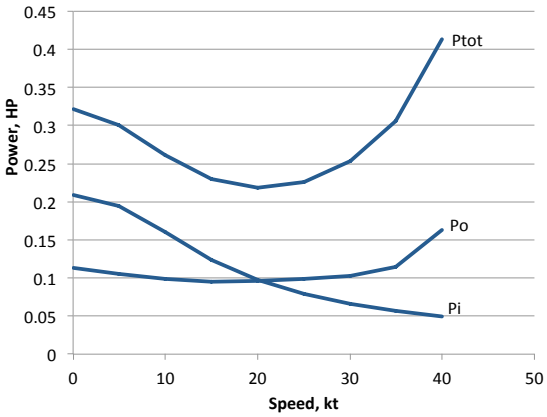

Figure 20. Power breakdown as a function of forward speed

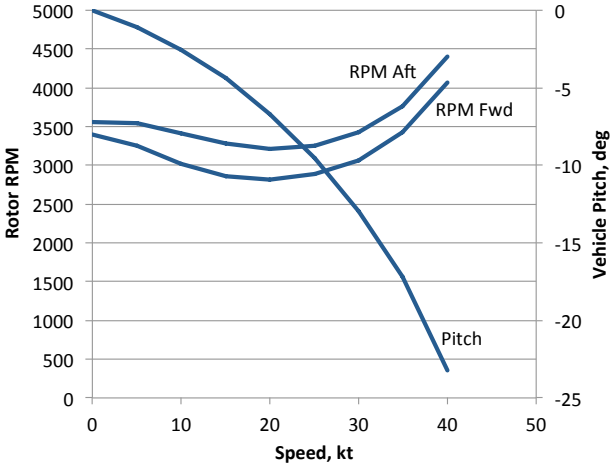

Figure 21. Trim variables as a function of forward speed

technology (110 Wh/kg, installed) gives a DGW of just over 6 lb for a 20-minute design mission. At this battery specific energy, the sizing process did not close for mission times above 20 min. Increasing the battery specific energy significantly increases the capability of the aircraft. At 400 Wh/kg, the mission time can be increased up to an hour, with a gross weight of only 5 lb.

Figure 23 shows the effect of payload weight on design gross weight for a number of different battery specific energy values. The effect of payload weight on design gross weight is approximately linear, with a slope depending on the level of battery technology. For a battery specific energy of 110 Wh/kg, the design gross weight increases approximately 4.5 lb per pound of payload. For the most optimistic prediction for battery technology shown (400 Wh/kg, installed), DGW only increases by 2 lb per pound of payload. The results also suggest that almost half of the benefit of a 400 Wh/kg battery can be attained by increasing the installed specific energy by just 40 Wh/kg, to 150 Wh/kg.

Many other sizing studies could be undertaken, but the simple variations shown in Figs. 22 and 23 should give an idea of the types of design studies that can be undertaken for sUAS using the NDARC software. The results shown in Fig. 20 suggest that longer flight endurance could be attained by flying the mission at 20 kt, rather than in a hover, which is the expected behavior based on traditional rotorcraft performance. The decision to alter the mission profile would of course have to consider whether persistent hover in a single location is necessary to accomplish the objectives of the mission.

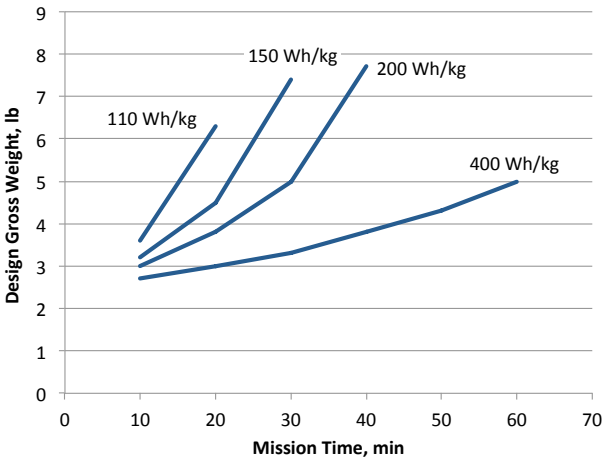

Figure 22. Design gross weight vs. mission time – 0.5 lb payload

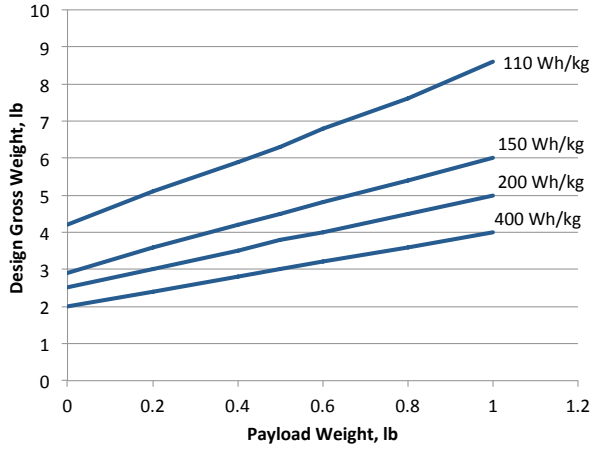

Figure 23. Design gross weight vs. payload – 20 min mission

SUMMARY AND CONCLUSIONS

This paper has demonstrated the feasibility of modeling and designing a sUAS quadcopter using the rotorcraft design software NDARC. The NDARC models were informed by a multi-component toolchain, including comprehensive analysis, experimental wind tunnel and hover test data, and vehicle component measurements.

Because the full-scale rotorcraft scaling models included with NDARC are not appropriate for sUAS, simplified scaling models for various components were developed based on measured values for existing aircraft. There is significant variation in sUAS components, so scaling laws should be based on hardware similar to what is being used for the application at hand.

Experimental performance data were used to adjust NDARC inputs to achieve more accurate results. Based on the results shown here, NDARC can predict hover performance very accurately, but was less successful in forward flight. Further tuning of the models may result in better matching to experimental data. For calculating rotor power, a higher fidelity analysis, such as CAMRAD II, is necessary to at least calculate the effect of thrust and tip speed on rotor and profile power coefficients in hover. The resulting $\varkappa$ and $c_{d,mean}$ values may be sufficient for low-speed flight, depending on the level of accuracy desired.

This study has shown the feasibility of using the NDARC toolchain to model and re-size quadrotor aircraft. By extension, using NDARC to model any multirotor configuration, such as hexacopters and octocopters, at this scale should be possible. Battery technology has a very large impact on vehicle sizing, and for current technology levels, batteries can represent almost half of the empty weight of the vehicle. As battery technology evolves towards higher energy densities, future sUAS will become much more capable.

This design study demonstrated the utility and capability of conceptual design tools, such as NDARC. These tools will enable sUAS designers to assess multiple vehicle iterations before building hardware, which should ultimately drive down development costs and improve vehicle capabilities. Furthermore, use of these tools can highlight deficiencies in current technologies and help guide the direction of future research in the improvement of small unmanned aircraft systems.

ACKNOWLEDGEMENTS

The authors would like to acknowledge the contributions and cooperation of Straight Up Imaging in providing details of the Endurance vehicle.

REFERENCES

1. Theodore, C., “A Summary of the NASA DELIVER Project,” AHS International Technical Meeting on Aeromechanics Design for Transformative Vertical Flight, San Francisco, CA, January 16-18, 2018.

2. Niemiec, R., Gandhi, F., and Singh, R., “Control and Performance Analysis of a Reconfigurable Multi-Copter,” AHS 73rd Annual Forum, Fort Worth, TX, May 9-11, 2017.

3. Beals, N., “Design of Small Rotors for Multicopter UAS,” AHS 73rd Annual Forum, Fort Worth, TX, May 9-11, 2017.

4. Russell, C. and Sekula, M., “Comprehensive Analysis Modeling of Small-Scale UAS Rotors,” AHS

International 73rd Annual Forum, Fort Worth, TX, May 9-11, 2017.

5. Johnson, W., "NDARC – NASA Design and Analysis of Rotorcraft Theoretical Basis and Architecture," AHS Aeromechanics Specialists' Conference, San Francisco, CA, January 20-22, 2010.
6. Johnson, W., "Propulsion System Models for Rotorcraft Conceptual Design," AHS 5th Decennial Aeromechanics Specialists' Conference, San Francisco, CA, January 22-24, 2014.
7. Johnson, W., Silva, C., and Solis, E., "Concept Vehicles for VTOL Air Taxi Operations," AHS International Technical Meeting on Aeromechanics Design for Transformative Vertical Flight, San Francisco, CA, January 16-18, 2018.
8. Russell, C., Jung, J., Willink, G., and Glasner, B., "Wind Tunnel and Hover Performance Test Results for Multicopter UAS Vehicles," AHS 72nd Annual Forum, West Palm Beach, FL, May 16-19, 2016.
9. "Products – Straight Up Imaging," http://www.straightupimaging.com/products/, accessed Dec. 10, 2017.